JOURNAL OF GEOPHYSICAL RESEARCH, VOL. 106, NO. D6, PAGES 5227–5238, MARCH 27, 2001

Comparison of upper tropospheric humidity retrievals from TOVS and Meteosat

Christelle Escoffier,[1] John J. Bates,[2] Alain Chédin,[3] William B. Rossow,[4] and Johannes Schmetz[5]

Abstract. Two different methods for retrieving upper tropospheric humidity (UTH) from the TIROS Operational Vertical Sounder (TOVS) instruments aboard NOAA polar orbiting satellites are presented and compared. The first one, from the Environmental Technology Laboratory, computed by J. J. Bates and D. L. Jackson, estimates UTH from a simplified radiative transfer analysis of the upper tropospheric infrared water vapor channel at 6.7 μm wavelength measured by High-resolution Infrared Radiation Sounder (HIRS). The second one results from a neural network analysis of the TOVS (HIRS and Microwave Sounding Unit (MSU)) data developed at the Laboratoire de Météorologie Dynamique. Although the two methods give very similar retrievals in temperate regions (30°-60°N and S), the latter is larger by up to 16% in the tropics. The two data sets have also been compared with the UTH retrievals from infrared radiance measurements at 6.3 μm wavelength from the geostationary satellite Meteosat. These products are taken from the archive without any reprocessing that would take care of known biases. Since the Meteosat UTH in 1989 was confined to clear-sky areas, it has a dry bias. The differences observed among the three data sets can be explained. UTH computation is sensitive to assumed air temperature and humidity profiles. Despite the biases the spatial and temporal correlations are very good. Overall, the comparison of the two TOVS retrievals provides an assessment of the UTH uncertainties, about 15-25% (relative). With regard to the Meteosat UTH it is concluded that the archived product performs well in depicting spatial and temporal changes. For future quantitative analyses, a reprocessing of the Meteosat UTH is suggested.

1. Introduction

One of the major controversies about atmospheric distribution of water vapor concerns its amount in the upper troposphere. Outgoing longwave radiation (OLR) fluxes are very sensitive to this quantity [*Spencer and Braswell,* 1997], especially in a dry atmosphere, so upper tropospheric humidity variations can have important effects on climate changes. Unfortunately, water vapor is poorly measured in the upper troposphere where radiosonde measurements are unreliable [*Elliott and Gaffen,* 1991; *Soden and Lanzante,* 1996]. Therefore water vapor measured from satellites is a way to add important information, especially since satellites provide the only globally complete analysis of humidity fields. Recent papers have described several data sets based on clear-sky infrared radiances from the moisture-sensitive channel onboard geostationary satellites [*Schmetz and Turpeinen,* 1988; *Turpeinen and Schmetz,* 1989; *Soden and Bretherton,* 1993] and polar orbiting satellites [*Bates et al.,* 1996; *Stephens et al.,* 1996; *Chaboureau et al.,* 1998]. Currently, the geostationary measurements provide information regarding the vertically averaged water vapor content of the upper troposphere (roughly 300-600 hPa), while the polar orbiter measurements describe the vertical distribution of the tropospheric moisture from the surface to about 100 hPa.

Several methods exist to retrieve water vapor amount in the upper troposphere from satellite infrared radiances. The different methods are usually dependent on ancillary data such as radiosondes or European Centre for Medium-Range Weather Forecasts (ECMWF) profiles. A comparison between different satellite retrievals is one way of evaluating the quality of the remote sens-

[1]Goddard Institute for Space Studies, Columbia University, New York, New York.

[2]NOAA ERL, Environmental Technology Laboratory, Boulder, Colorado.

[3]Laboratoire de Météorologie Dynamique, Palaiseau, France.

[4]NASA Goddard Institute for Space Studies, New York, New York.

[5]European organisation for the exploitation of meteorological satellites, Darmstadt, Germany.

Paper number 2000JD900553.
0148-0227/01/2000JD900553$09.00

ing observations. In this study we compare three of the most extensive data sets of upper tropospheric humidity (UTH) retrieved from satellites (described in section 2) in order to assess current uncertainties. Since we use the Meteosat observations, the domain of study is restricted to the Meteosat view of the Earth, centered at 0°W,0°N, with a 55° latitude-longitude radius. A physical retrieval method, based on a neural network approach, is compared to two analytical methods based on a simplified radiative transfer theory to relate brigthness temperature to relative humidity. Perfect agreement is not expected yet because algorithms, spectral channels, and the upper tropospheric layers observed are slightly different. The results of the comparisons are described in the section 3. In section 5, we try to explain the systematic differences.

2. Data Description

The quantity UTH is defined as the weighting function averaged relative humidity computed over a deep layer of the upper troposphere between 200 and 600 hPa in a simple relationship to infrared brightness temperature (T_b) measured by both TIROS-N Operational Vertical Sounder (TOVS) channel 12 (6.7 μm wavelength) and the Meteosat water vapor channel (6.3 μm wavelength). Such channels are sensitive both to air temperature and to moisture in the upper troposphere, which explains the interpretation of T_b in terms of relative humidity, which is also a function of temperature and specific humidity. The following study is done for 4 months in 1989 (January, April, July, and October) in the Meteosat domain. The year 1989 was selected as an example within the 1987-1995 common coverage period of the three data sets. The Meteosat image is subdivided into segments of 32 x 32 IR pixels, corresponding to about 160 x 160 km at the subsatellite point or about 200 x 200 km on average. The other data sets used in this study are averaged on the same grid. UTH retrievals are available from Meteosat only twice daily (1100 and 2300 LT), whereas four retrievals, two from NOAA 10 (0730 and 1930 LT) and two from NOAA 11 (0230 and 1430 LT), are mixed to compute UTH in both TOVS data sets. The temporal resolutions examined are 5 days (pentads) and monthly averages.

In the following, the three UTH data sets are defined and the relative humidity in percent is calculated with respect to liquid water. Percent values will also represent absolute differences of relative humidity or relative differences of relative humidity, as indicated in the text.

2.1. UTH From TOVS/HIRS, A Simple T_b Interpretation

This first UTH data set is from the Environmental Technology Laboratory and was computed by J. J. Bates and D. L. Jackson (BJ-UTH). The computation uses TOVS/HIRS (TIROS-N Operational Vertical Sounder/High-resolution Infrared Radiation Sounder) radiances from channels 12 (6.7 μm), 4 (14.2 μm), and 6 (13.7 μm). Channels 4 and 6 are used for operational temperature sounding (T_4 and T_6), whereas channel 12 (T_{12}) is sensitive to water vapor and air temperature in the upper troposphere. The radiances are limb corrected and cloud cleared by the operational NESDIS (National Environmental Satellite Data and Information Service) TOVS processing package [*Werbowetzki,* 1981; *Kidwell,* 1991]. The UTH retrieval method is based on the work by *Soden and Bretherton* [1993], using forward radiative transfer simulation, with some changes according to *Stephens et al.* [1996]. The water vapor channel brightness temperature T_{12} is interpreted as UTH, which is supposed to be the relative humidity in the 300-500 hPa layer, using

$$\log\left(\frac{< \mathrm{UTH} >}{< \beta >}\right) = \mathrm{a} + \mathrm{b}\mathrm{T}_{12}, \qquad (1)$$

where $< . >$ stands for the vertical average of a quantity. $< \beta >$ is a function of the difference (T_6-T_4) as shown by *Stephens et al.* [1996, Figure 11], except that the factor $\cos\theta$ is equal to 1, since angular corrections were applied to the radiance data.

Minor changes have been introduced by D. L. Jackson (personal communication, 1999), such as using temperature and humidity profile information from the climatological database TIGR-3 [*Chédin et al.,* 1985; *Chevallier et al.,* 1998] instead of TIGR-2, changing the Malkmus [*Malkmus,* 1967] radiative transfer model for the MODTRAN [*Berk et al.,* 1989] model and basing the weighting function on temperature profiles instead of atmospheric transmission profiles (in order to allow the weighting function to stay in the upper troposphere for most profiles). An uncertainty of approximately 15-20% (relative error) is estimated for this UTH product [*Stephens et al.,* 1996], but larger uncertainties exist poleward of 45°. This is a limitation of the method, which has difficulty retrieving UTH when air temperature is too low.

The BJ-UTH values have been constrained in order to avoid relative humidities with respect to ice greater than 100%, which leads the UTH values with respect to water (BJ-UTH product) smaller than 70%, a threshold observed in the data (see section 3).

2.2. UTH From Meteosat, A Simple T_b Interpretation

The radiances come from the water vapor (WV) channel of Meteosat, sensitive to radiation between 5.7 and 7.1 μm. In this study the Meteosat UTH products (Met-UTH) are taken from the archive at EUMETSAT and thus reflect the state of the retrieval algorithm in 1989. Then the retrieval was based on a look-up table derived from radiative transfer calculations for a set of fixed UTH values. The ECMWF forecast temperature profiles (from surface to 100 hPa) and ECMWF forecast humidity profiles (from surface to 600 hPa)

are used in the method to specify atmospheric structure. Between 300 and 600 hPa the humidity profile is varied, and above 300 hPa, humidity decreases linearly to 0% at 100 hPa. With these profiles, spectral radiances are calculated with an efficient radiative transfer model to produce a look-up table. The absolute error of this UTH product is estimated to be about 10-15% [*Schmetz and Turpeinen,* 1988]. However, the characteristics of the Met-UTH product are to a large extent determined by the selection of the clear-sky radiances used in the retrieval and satellite calibration. These have been greatly improved since 1989. Therefore it is important to note that the Met-UTH product used here is what is currently in the EUMETSAT archive. The salient features of the 1989 Met-UTH are as follows:

1. The Met-UTH was confined to retrievals in segment areas (32 x 32 pixels) which were completely free of medium- and high-level clouds. Obviously, this induces a dry bias that may exceed 30% (absolute) in moist regions. The reason for this procedure was that a "clean" comparison with radiosonde was desired; in partly cloudy areas this would not have been possible because a radiosonde could have traveled through the cloudy air, while the satellite radiance would not account for this. A climatology of such a Met-UTH product has been described by *van de Berg et al.* [1991].

2. The Met-UTH product suffered from a bias in the calibration which has been overcome, at least to a large extent, by the changes described by *van de Berg et al.* [1995]. Thus the comparisons with the mean Met-UTH is valuable only in a qualitative sense. More recent analyses [*Schmetz et al.,* 1995] were based on reprocessed data sets, which included various improvements.

2.3. UTH From TOVS/HIRS: A Neural Network Approach

UTH is computed from the precipitable water amount in the 300-500 hPa layer retrieved with the Improved Initialization Inversion (3I) method [*Chédin et al.,* 1985; *Scott et al.,* 1999] applied to NOAA-TOVS radiances (hereinafter called 3I-UTH). This water vapor data set is provided by the Laboratoire de Météorologie Dynamique (LMD). As for the BJ-UTH, the level 1B satellite radiance data are calibrated using coefficients provided by NOAA following the procedures set forth by *Kidwell,* [1991]. The 3I method to retrieve atmospheric, cloud, and surface variables is a physico-statistical method based on a pattern recognition approach. After determination of the temperature profile, cloud amount along with cloud top pressure and temperature are estimated using the procedure described by *Wahiche et al.* [1986] and improved by *Stubenrauch et al.* [1996, 1999]. The HIRS radiances in channels sensitive to water vapor, HIRS 8(11.1 μm), HIRS 10(8.3 μm), HIRS 11(7.3 μm), and HIRS 12(6.7 μm) and in the window channels are then corrected for the effects of partial cloud cover, making use of the previously determined cloud parameters. No cloud correction is attempted if the effective cloud amount is larger than 60%. Precipitable water amounts (above the surface to 100 hPa and above the 850, 700, 500, and 300 hPa levels to 100 hPa) are then retrieved using a nonlinear neural network approach [*Chaboureau et al.,* 1998]. The neural network is trained using the atmospheric profiles from the TIGR-3 database as outputs and the corresponding radiances calculated from the "4A" (Automatized Atmospheric Absorption Atlas [*Scott and Chédin,* 1981]) model as inputs.

To compare with Met-UTH or BJ-UTH products, the 3I precipitable water amount in the 300-500 hPa layer has to be transformed into UTH. As the transformation is strongly sensitive to air temperature (see section 4.2), the 3I-UTH has been calculated using daily retrieved precipitable water amount and temperature for the 300-500 hPa layer and then averaged 5 day or monthly values. The saturated vapor pressure has been calculated with respect to liquid water at three levels within the 300-500 hPa layer to have more accurate UTH results (since UTH is not exactly uniform in the 300-500 hPa layer).

3. Results

3.1. Spatial Variability

Figure 1 presents scatterplots in the tropical portion of the Meteosat view which compare the spatial variations of three UTH data sets. The 3I-UTH is more humid for tropical regions (best linear fit slopes larger than 1 when compared with BJ-UTH and Met-UTH) and Met-UTH is the driest. The larger dynamical range for the 3I-UTH results in a much better agreement in the dry regions than in humid regions. Despite the biases observed, the three data sets show very similar spatial patterns. Indeed, the spatial correlations are larger than 0.95 with an UTH standard deviation smaller than 6.5% (absolute). Two out of the four months in Table 1 (January and April) show smaller correlations in the comparison with Meteosat (0.92-0.94) and greater standard deviations of about 7% (absolute), which is not surprising in view of the known shortcomings of this data set. Note that the January/April 1989 UTH is based on Meteosat 3 observations, while July/October 1989 used Meteosat 4, which had an improved water vapor channel (e.g., 8 bit digitization).

The temperate regions (30°-60°N and S) are drier overall than the tropical regions; the 3I-UTH data set shows this difference very well. In the midlatitude regions the correlation between the data sets are always larger than 0.98 with an UTH standard deviation smaller than 3.5% (absolute), as shown in Table 2, except for the comparisons with BJ-UTH in January and July. This discrepancy between the BJ-UTH and the other two data sets is also observed in the scatterplots of Figure 2 and appears mostly at higher latitudes in the winter hemisphere (north in January and south in July), where BJ-UTH becomes larger than the other two data

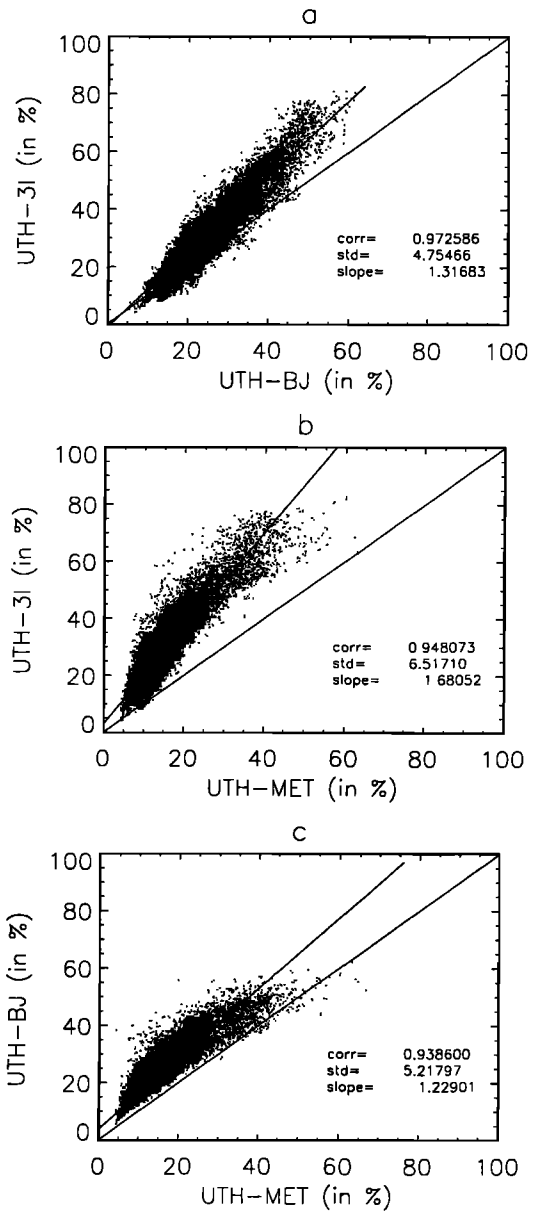

Figure 1. Scatterplots in the tropical regions (30°N-30°S) of Meteosat view for January, April, July, and October (4 months in the same plot): (a) 3I versus BJ, (b) 3I versus Met, and (c) BJ versus Met. The c stands for correlation and std for standard deviation.

Table 1. Correlation and Standard Deviation (in Percentage, in Parentheses) for the Four Months of Each Scatterplot of Figure 1 in the 30°S-30°N Band of the Meteosat View

	3I/BJ	3I/Met	BJ/Met
January	0.97(4.8)	0.93(7.5)	0.92(6.4)
April	0.98(3.9)	0.94(6.6)	0.94(5.1)
July	0.97(4.7)	0.97(4.8)	0.97(3.3)
October	0.97(4.7)	0.97(5.2)	0.96(4.3)

Each column represents a two data set comparison (2600 values).

Table 2. Same as Table 1 in the 30°-60°N and S Band, Corresponding to Figure 2 (900 Values)

	3I/BJ	3I/Met	BJ/Met
January	0.95(4.6)	0.98(3.0)	0.96(4.4)
April	0.98(3.2)	0.98(3.4)	0.98(3.1)
July	0.95(4.4)	0.99(2.2)	0.95(4.9)
October	0.99(2.4)	0.99(2.8)	0.98(3.3)

sets. The limitation of the BJ method to retrieve UTH only when air temperatures are large has been stressed in the description of this method. BJ-UTH and 3I-UTH have the best agreement, 3I-UTH being a little larger

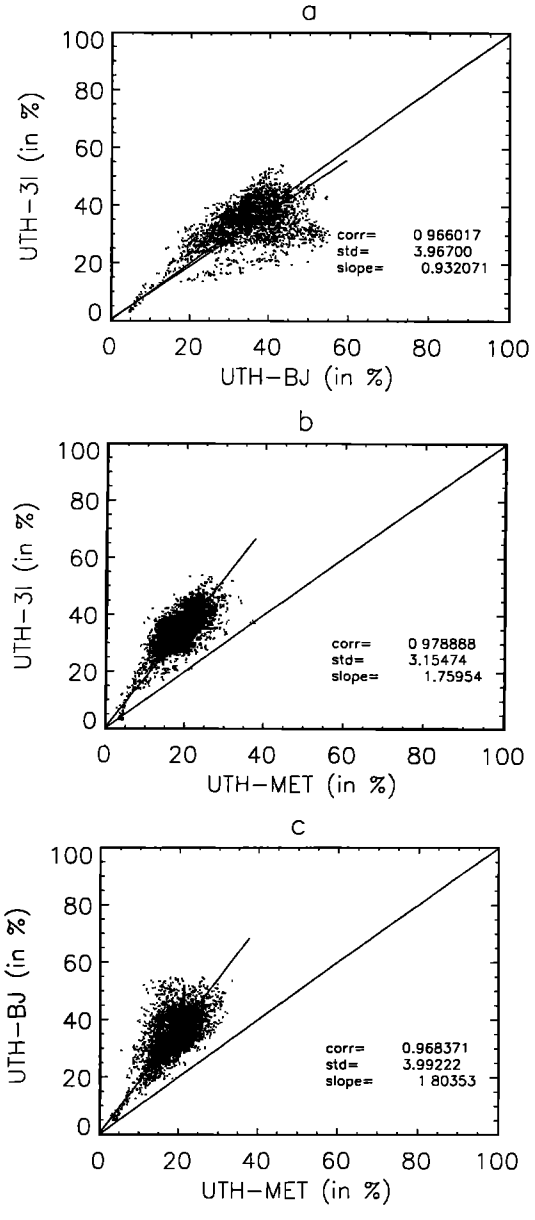

Figure 2. Same as Figure 1 in the midlatitude regions (30°-60°N and 30°-60°S).

between 30° and 40° (N and S) and BJ-UTH larger between 40° and 60° (N and S). Met-UTH is always much smaller than both TOVS retrievals; the best linear fit slope is between 1.76 and 1.80.

Figure 3 illustrates the differences of spatial patterns between each data set and the mean of the three (only July is shown). Each UTH data set is in agreement with the mean to within 7% (absolute) in the dry regions and within 21% (absolute) in the more humid regions, UTH-3I being wetter and Met-UTH drier. The BJ-UTH is in agreement within 7% (absolute difference) over the whole region, except in the winter at high latitudes where it is more humid by up to 20% (absolute). A 7% absolute bias in dry regions and a 21% absolute bias in humid regions represents a relative bias to the mean of more than 30% in both regions. The absolute difference between the two TOVS (BJ and 3I) UTH data sets is $\leq$ 4% in dry regions and $\leq$ 12% in humid regions, up to 15% in very humid zones (not shown). The relative bias to the mean in this case is about 15%, between 20 and 25% in very humid and very dry regions. The latter differences might be a better estimate of the current uncertainties in satellite UTH values because of known problems into the 1989 Met-UTH.

In conclusion, the three data sets, are very well correlated spatially but exhibit systematic discrepancies in the magnitude of the mean variation from humid to dry conditions. Indeed, the range of average humidities suggests UTH uncertainties of more than 30% (less than 25% if only the two TOVS UTH are considered), despite the fact that the accuracy of each data set has been estimated to be about 10 to 20% (relative error).

The best spatial correlation for the four months is observed between BJ and 3I in tropical regions and between Met and 3I in midlatitudes. The best relative humidity agreement is observed between BJ and Met in tropical regions and between 3I and BJ in midlatitudes. Since the spatial correlation is rather good, it is worth looking more carefully at the temporal variability, using monthly and 5-day means.

3.2. Temporal Variability

Variations on two timescales are explored. Figure 4 shows the monthly differences of zonal means (every 5° latitude) UTH between summer and winter months and between autumn and spring months, approximating the annual cycle amplitude in the three data sets. The Meteosat view is divided into two parts, the west part be-

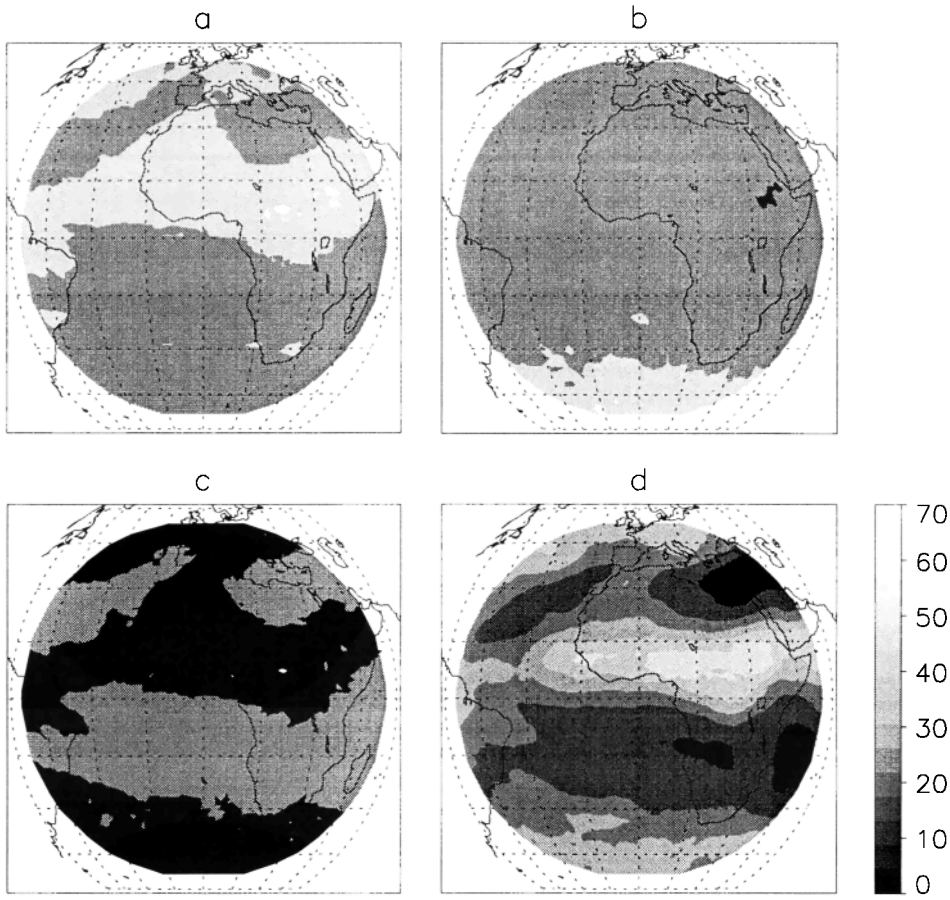

Figure 3. UTH difference (in percentage) between the data sets (a) 3I, (b) BJ, (c) Met and the mean of the three in July. For clarity, note that light gray is between +21 and +7%; gray is between +7 and -7%; and black is between -7 and -21%. (d) Average of the three data sets in July 1989 (in percentage).

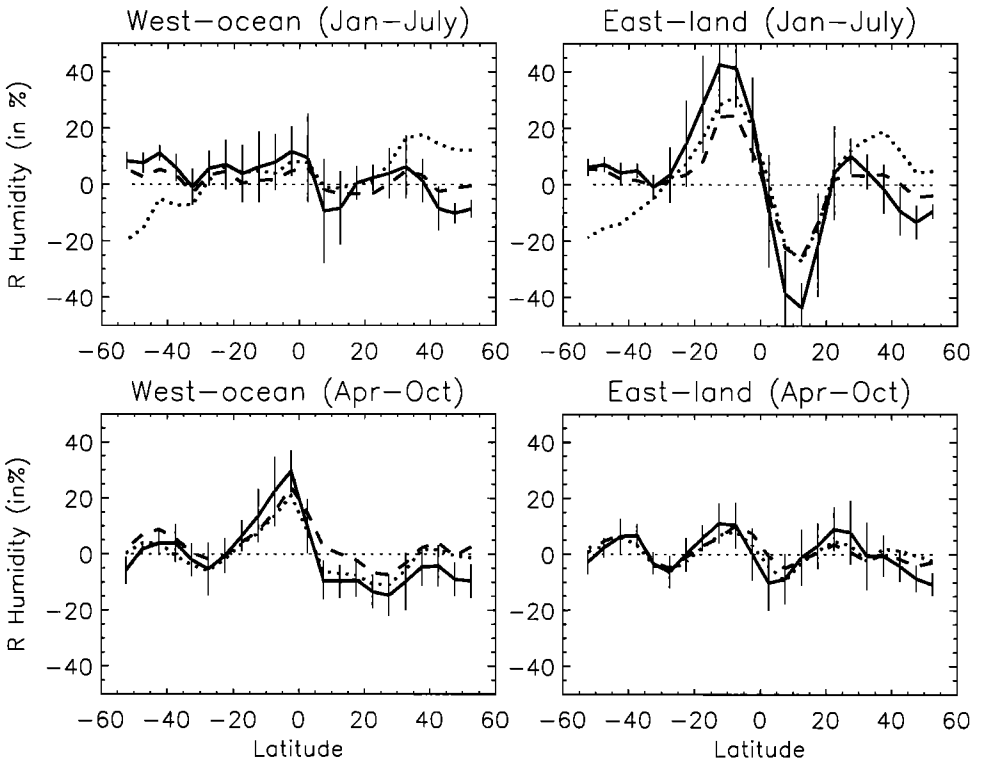

Figure 4. Monthly differences of UTH zonal mean average on every 5° of latitude over the west part (left) and the east part (right) of the Meteosat view. (top) January-July differences; (bottom) April-October differences. Negative latitude are for Southern Hemisphere. The standard deviations to the zonal mean (error bar) are shown for 3I only; 3I, solid line, BJ, dotted line, and Met, dashed line.

ing dominated by ocean (Figure 4 left) and the east part by land (Figure 4 right). Error bars represent the zonal mean standard deviations for the 3I data set (which has the largest variability). The January-July difference is significant over land, showing the seasonal movement of the Intertropical Convergence Zone (ITCZ) across the equator. On the sea (Figure 4 left) the January-July difference is not significant compared to the error bars. The ITCZ has less variability over sea than over land, as is also shown by precipitation analyses and water vapor data in the work of *Peixoto and Oort* [1992].

The April-October difference has a significant positive maximum in the southern tropical ocean (west part), which is not observed on land and which is linked to a large relative humidity and precipitation rate east of Brazil over the southern Atlantic Ocean in April. This feature has also been observed by *Peixoto and Oort* [1992] in other data sets.

In general, the zonal mean correlation among the three data sets is good (larger than 0.8, except for the January-July over ocean). The 3I-UTH presents slightly larger amplitude but not significantly, compared to the error bar. The annual amplitudes given by the three data sets are similar (35% ±15% for January-July over land and 25% ±10% for April-October over sea).

We select four regions of 15° latitude by 15° longitude in the Meteosat view as shown in Figure 5. Regions A and B are in the tropical zone (15°N-15°S). Region A is definitely in a subsidence region, while region B has its relative humidity amount varying with ITCZ movement. Regions C and D are located northward and centered at latitudes 22.5°N (region C) and 37.5°N (region

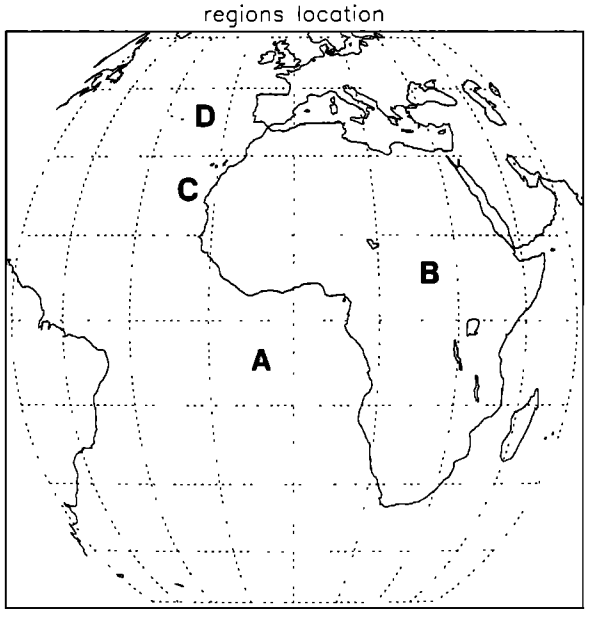

Figure 5. Position of the four [15° latitude x 15° longitude] regions described in the text. The latitude-longitude grid shows limits of the four following boxes: Region A, B, C, and D.

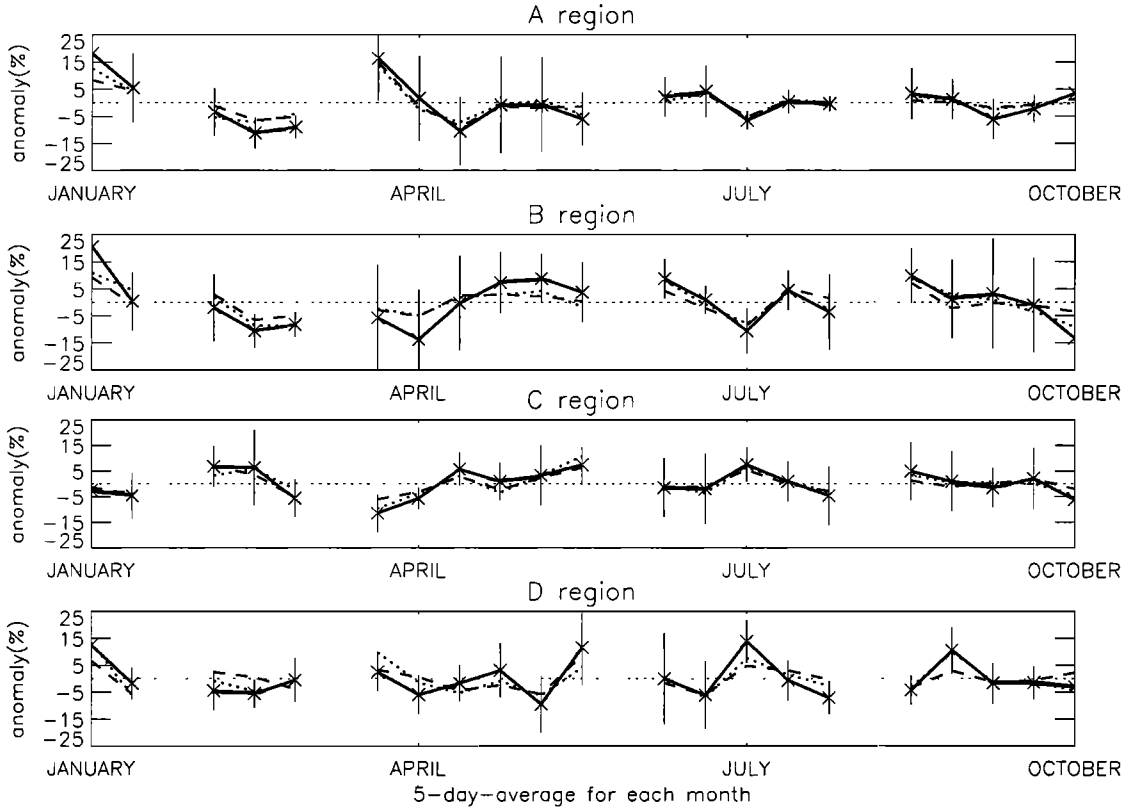

Figure 6. Five-day-average anomalies time series plotted for the four selected regions of Figure 5: 3I, solid line, BJ, dotted line, and Met, dashed line.

D). We focus on 5 day average anomaly time series plotted in Figure 6. For a given UTH method the anomalies are defined as 5 day average minus the mean for the corresponding month. The anomaly calculation eliminates the biases among the three data sets and shows intramonthly anomalies. The third pentad of 1989 is missing since no data were available in the NESDIS TOVS operational data for this period. In region A the 5 day average correlation is very good (Table 3). In region B, 3I-UTH has significantly larger anomalies in April and January but is still well correlated with the other two data sets (Figure 6). In the northern region D, where the variations are smaller, the correlation is the worst but still good (0.6-0.7), as shown in Table 3. The error bars represent the spatial standard deviations of the mean. The rms differences among the data sets vary from 5% (absolute) between BJ-UTH and Met-UTH in dry tropical region A to 23% (absolute) between 3I-UTH and Met-UTH in humid tropical region B (Table 3). Despite the large biases the temporal variations of the three data sets are in excellent agreement within the error bars in the four regions. Thus the intramonthly anomalies determined from all three data sets appear to be reliable.

Table 3. Correlation and RMS (in Percentage, in Parentheses) in Four Different Regions Shown in Figure 5

	3I/BJ	3I/Met	BJ/Met
Region A	0.96(6.0)	0.93(9.7)	0.96(5.0)
Region B	0.95(15.6)	0.96(23.6)	0.96(9.1)
Region C	0.90(6.8)	0.90(15.7)	0.87 (9.6)
Region D	0.76(5.9)	0.62(17.7)	0.78(16.8)

The correlation and rms are calculated with 5-day-averaged time series (plotted in Figure 6) over the following months: January, April, July, and October 1989. Each column represents a two data set comparison (20 values).

Figure 7 is a space-time Taylor diagram which summarizes the spatial-temporal agreement among the three data sets. Here anomalies are defined with respect to a spatial-temporal mean, calculated with all pentad time series of the region considered (regions A, B, C, D or the whole Meteosat view). The 3I-UTH, which has the largest average humidity and variations, has been chosen as the reference data set. The circle identified by 1 is the variance normalized to the reference data set variance. Data plotted near this circle have similar amplitude variations as the reference data; data closer to the center have smaller amplitudes. The angle with respect to the Y axis represents the correlation with the reference data set. High correlations are closer to the X axis, and low correlations are closer to the Y axis. The 3I-UTH has the largest space-time variance (all points are within the circle = 1), except in region D where BJ-UTH has a slightly greater amplitude. Met-UTH has

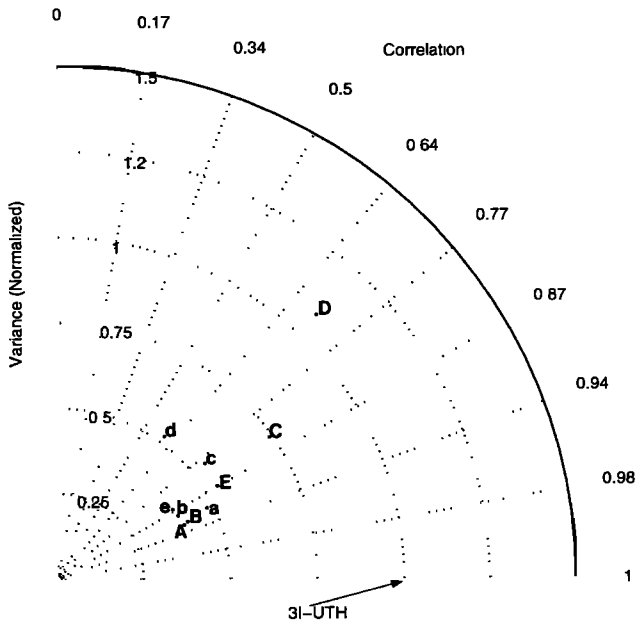

Figure 7. Taylor diagram: Space-time variance of UTH in four regions and the global Meteosat view by BJ and Met with 3I as reference. The radial coordinate gives the magnitude of total variance normalized to the reference data set, and the polar coordinate gives the correlation with the reference data set. A, B, C and D represent the respective regions plotted in Figure 5. E stands for the Meteosat view. Capital letters stand for BJ data set and small letters for Met data set.

the smallest variance, except in the subsidence region A where BJ-UTH shows lower variance. A decrease of the space-time correlations with latitude is observed (Figure 7). In tropical regions the correlation is between 0.87 and 0.94, in region C between 0.77 and 0.87, and smaller than 0.64 in region D. A "global" correlation of about 0.87 is found for the whole Meteosat view.

4. Can the Bias Among the Three Data Sets Be Explained?

According to the results of section 3, a systematic disagreement is observed in the relative humidity amounts and in the time-space variances. We try to explain these discrepancies.

4.1. Weighting Function

The 3I-UTH provides values larger than the other two data sets in the convective zones but similar in the subsidence zones. The 3I-UTH values are for the 300-500 hPa layer whatever the region observed and its conditions, whereas the precise layer represented by the other two methods depends on the weighting functions, which depend on both the water vapor amount and the temperature vertical profiles. The maximum of the weighting function shifts from about 300 hPa for a wet tropical profile to about 500 hPa for a dry tropical profile (Figure 8). The maximum of the weighting func-

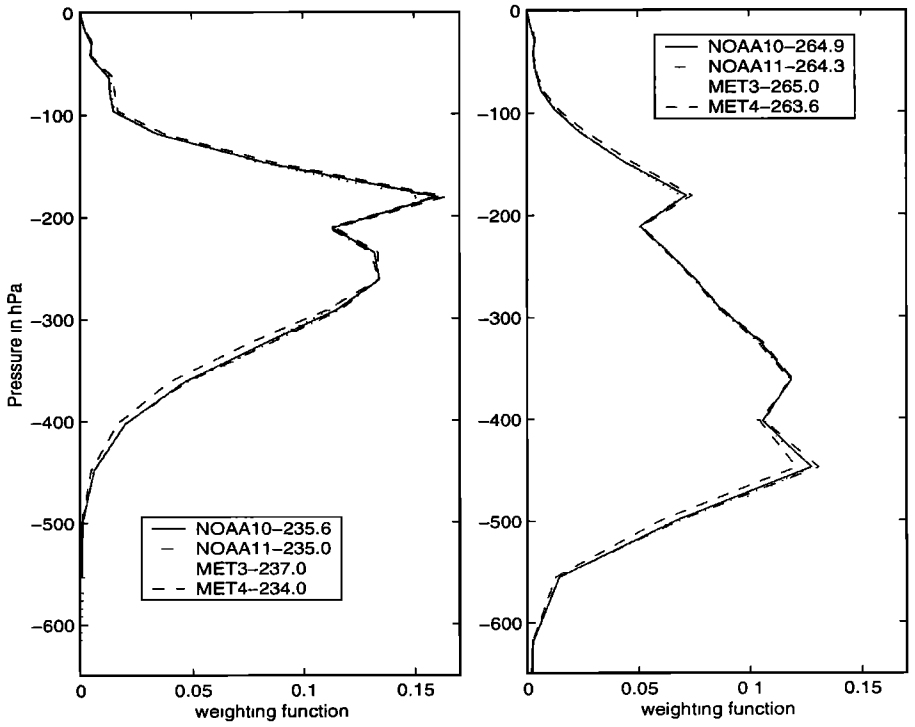

Figure 8. Water vapor channel weighting function of four satellites (Met 3, Met 4, NOAA 10, and NOAA 11) for two profiles: (left) a humid profile (300-500 hPa humidity of 100%, 300-500 hPa water vapor content of 1.26 cm, air temperature between 246° and 270°K); (right) a dry profile (300-500 hPa humidity of 1%, 300-500 hPa water vapor content of 0.0064 cm, air temperature between 235° and 263°K). Corresponding brightness temperatures follow the name of the satellite.

tion also depends on the view angle of the satellite. In humid cases the BJ and Met methods measure UTH in a layer slightly above the 300-500 hPa layer and lower in dry cases. Thus the relative humidity amount measured by these two methods is different than measured by the 3I method depending on the profile. The effect of the shifting weighting function is to reduce the magnitude of the difference of UTH between wetter and drier profiles, which explains the larger dynamical range of 3I-UTH.

Using the 4A radiative transfer model, we calculated the brightness temperatures corresponding to all the TIGR-3 profiles for the four following water vapor channels: channel 12 (centered at 6.7 μm) for HIRS on NOAA 10 and NOAA 11 and the water vapor channel (centered at 6.3 μm) for Met 3 and Met 4. Two examples are plotted in Figure 8, one for a dry profile and one for a humid profile. Although the instrument spectral response function shapes are very different, the weighting functions plotted in Figure 8 are nearly the same, but the same water vapor amounts correspond to different brightness temperatures. The bias between brightness temperatures from Met 3 and Met 4 is about 3°K. These differences are taken care of in the calibration and the physical Met-UTH retrieval, which considers the spectral response functions in the radiative model calculations. Thus UTH from Met 3 and Met 4 in the present study are not much different. The absolute difference between Meteosat and NOAA-TOVS brightness temperature is about 1.5°K. These brightness temperature discrepancies are observed for all the TIGR-3 profiles.

4.2. Air Temperature Sensitivity of the Transformation From Precipitable Water Amount to Relative Humidity

To illustrate the sensitivity to air temperature of the conversion of the 3I precipitable water vapor amount to UTH, we performed three experiments. In the first experiment the 3I precipitable water amount is transformed into UTH using 3I-retrieved air temperature (UTH_t) and this value +1°K (UTH_{t+1}). The 1°K difference, which corresponds to a 0.5% relative error in air temperature, introduces more than 10% relative error in UTH (not shown). This result is in agreement with *Peixoto and Oort* [1996] who show that 1% variation on air temperature can induce more than 20% relative error in UTH.

The sensitivity of the transformation to air temperature errors is emphasized in a second experiment, which consists of comparing two 3I-UTH products: the first product (UTH_d) is transformed from daily precipitable water amount and daily air temperature, then averaged over the month. The second product (UTH_m) is transformed using the monthly mean values of precipitable water amount and air temperature. Table 4 shows the difference between these two products. UTH_m is systematically larger than UTH_d by 4% (absolute). This effect results from the fact that the monthly average air temperature is less variable by about 0.5% compared to daily air temperature and in this way produces the 4% absolute difference in UTH.

The last sensitivity test uses two different saturated vapor pressures. Air temperature averaged over the 300-500 hPa layer is used to calculate the first saturated vapor pressure (ew_1). Air temperatures derived at three different levels (300, 400, and 500hPa) give three saturated vapor pressures, which are then averaged over the whole layer (ew_3). The UTH data set calculated with ew_3 is systematically drier than the UTH data set calculated with ew_1. The largest absolute bias, between 12 and 20%, is observed in regions poleward of 40°, where the temperature is the coldest and UTH more sensitive to temperature variations. In the tropical band between 30°N and 30°S the absolute bias is smaller than 3-6%. The variability of temperature in the tropical band is relatively small.

The tests applied to 3I-UTH show that a 1% relative error of air temperature can induce more than 10% relative error of UTH. Likewise, a small variation of air temperature within the 300-500 hPa layer can induce significant change in saturated vapor pressure and so in the UTH retrieval. The third test stresses the sensitivity in very low temperature cases because the largest absolute biases are observed at high latitudes.

4.3. Cloudy Regions and Calibration in Met-UTH Algorithm

As shown by *Gaffen and Elliott* [1993], the climatological column water vapor content in the lower troposphere (surface to 400 hPa) for clear-skies is smaller than for cloudy-skies. The difference is about 10 to 15% (relative) in tropical regions and can be larger in midlatitude zones. An explanation for Met-UTH products providing values smaller than the other two TOVS data sets (best linear fit slopes larger than 1 both compared with BJ-UTH and 3I-UTH) could be caused by the particular UTH retrieval algorithm in operation at that time. As mentioned above, in 1989 the Met-UTH operational product was derived only for "large" areas

Table 4. Absolute RMS and Bias (UTH_m-UTH_d) for Four Months of 1989

Months	January	April	July	October
RMS	4.0	5.5	4.3	4.7
Bias	-3.2	-4.7	-2.8	-3.7

UTH_m stands for 3I relative humidity computed with water vapor content and air temperature monthly means and UTH_d for 3I relative humidity computed with daily values and monthly averaged afterward. The region is only the Meteosat view.

of 32 x 32 pixels free of cloud at pressures smaller than 700 hPa. Thus the clear radiances mixed with cloudy values were not used to derive UTH. This could make the product a lot drier since we avoid cloud-free areas in the proximity of clouds and could also reduce the dynamic range of Met-UTH product. A later change (after 1989) in the Met-UTH product includes clear radiances from partly cloudy regions and leads to a large increase in the dynamic range, as shown in the following comparison: Figure 5 of *van de Berg et al.* [1991], before the change compared to Figure 5 of *Schmetz et al.* [1995] after the change, exhibits a 20% absolute difference in the convective zone humidity. Thus an absolute bias of at least 20% in moist regions could be explained by excluding clear radiances from partly cloudy regions in Met-UTH retrieval.

A bias between Met-UTH and the two TOVS UTH is also observed in dry regions. The offset observed in Figure 1 between Met-UTH and BJ-UTH is probably induced by a calibration bias. Indeed, *van de Berg et al.* [1995] proposed a new calibration of Meteosat radiances, which decreases the radiances by 8% (relative), and so increases Met-UTH accordingly. The bias correction in the UTH depends on the UTH value.

The Met-UTH algorithm has been improved over time, so UTH products from the archive are not homogeneous. An important suggestion from this study is that future studies of the UTH product should be based on a reprocessing with a state-of-the-art algorithm and retrieval method and not based on the currently archived data. The salient point of this section is that in view of the known characteristics of the Met-UTH of 1989 (avoidance of partially cloudy regions and calibration bias), any discussion of a bias of the Met-UTH is premature.

5. Conclusion

In the present study, three upper tropospheric humidity (UTH) data sets retrieved from satellite measurements have been compared. The retrieval characteristics depend on the satellite radiance calibration, the retrieval algorithms, and all additional assumptions, particularly regarding the constancy of the vertical profiles of temperature and humidity.

Comparison of each data set to the mean of the three gives a range of values of 20% (absolute) in the convective zone and 7% (absolute) in the arid zones. Using only the two TOVS UTH values, the range decreases to 15% (absolute) in very moist regions and 4% in dry regions. Such a range is significant (relative difference to the mean of the three data sets is more than 30% and about 15-25% for only the two TOVS) compared to the published uncertainty estimates for the UTH retrievals (relative uncertainties of 15-20%). Different explanations for the discrepancies were investigated.

We note the difference between the UTH quantity and the relative humidity in the 300-500 hPa layer. By definition, UTH is directly related to the 6.7 μm brightness temperature but interpreted in terms of the relative humidity in a broad layer (about 200-500 hPa); however, the precise limits of the layer represented vary depending on the air temperature, the specific humidity profile, and the view angle of the satellite as we have shown. In other words, there is a systematic shift in the layer altitude with humidity which can reduce the magnitude of humidity changes. In contrast, the 3I method retrieves the relative humidity in a fixed layer, 300-500 hPa, which is not the same as UTH. The difficulty of computing UTH derived from precipitable water vapor content has also been emphasized and is mainly due to the conversion sensitivity to air temperature. Concerning the Met-UTH and in view of the known characteristics of this Met-UTH product of 1989 (avoidance of partially cloudy regions and calibration bias), it can be stated that any discussion of a bias of the Met-UTH is premature. Spatial and temporal variability, however, are captured by Met-UTH consistent with the variability shown by the two TOVS products.

All three methods use ancillary data to evaluate the model and to follow the evolution of the sensor throughout its lifetime. Given the inaccuracy of the radiosonde observations of humidity in the upper troposphere [*Elliott and Gaffen,* 1991; *Soden and Lanzante,* 1996], reliance on them may introduce problems. Several studies [*Eyre,* 1987; *Reuter et al.,* 1988] also illustrate the impacts that ancillary data, as radiosonde observations, can have on the final retrievals. The errors introduced in this way in the three methods are hard to quantify.

The spatial and temporal correlations among the three methods is very high, around 0.9 for the spatial correlation and 0.85 for the time-space correlation. The 3I-UTH shows larger variability than the other two data sets; the lower variability of Met-UTH and BJ-UTH could come from the variation of the weighting function peak altitude with humidity (section 4.1).

The present comparison gives the uncertainty of relative humidity in the upper troposphere retrieved by satellite (based on the 1989 year). The range of systematic differences is more than 30% (relative), which is largely explained by known differences in the product characteristics. Future reprocessing with a state-of-the-art algorithm and retrieval should significantly diminish these biases. This is especially true for the Met-UTH product which was taken from the archive and thus reflects the retrieval implementation as of 1989. An assessement of the "current" uncertainty of UTH from satellite using only the two TOVS data sets suggests that it is about 15-25% (relative), which is slightly larger than previous estimates. This study underlines the importance of the details of each method for computing UTH. The high correlation (larger than 0.8) both in space and in time gives confidence in the UTH variability results and encourages us to believe that additional work to understand the relative merits of each method may produce a consensus algorithm and a more

accurate product. It should also be noted that the existence of biases between different satellites and different methods of estimating UTH does not represent a fundamental limitation in the quantitative use of UTH for climate applications. Instead, it indicates the need for a careful program of intercalibration of satellite water vapor radiance channels and of UTH methods. In spite of the progress made over the last decade, recent work examining satellite calibration [*Bréon et al.,* 1999] and satellite intercalibration [*Bréon et al.,* 2000; *Sohn et al.,* 2000] have revealed significant biases, but these biases are currently being worked on. Similarly, a program to intercompare methods to retrieve UTH has been started. Early results of these intercomparison programs indicate that the biases found in this present analysis are likely to be reduced, even beyond the known sources of biases discussed in this paper. Careful intercalibration of the different instruments and different UTH methods will be required to achieve this goal. More extensive results on these programs will be reported in future articles.

Acknowledgments. This work was funded by NASA as an augmentation to the NOAA NASA Enhanced Data Sets Program and as a contribution to the Global Energy and Water Cycle Experiment (GEWEX). Partial funding has also been received from EUMETSAT. This work was also supported by NOAA and LMD. The BJ-UTH products were provided by D. L. Jackson, the 3I-UTH products by the "Analyse du Rayonnement Atmospherique" team from LMD and the Met-UTH products by EUMETSAT. We would like to thank M. Koenig for her help to access Meteosat data. Thanks are due to S. Tjemkes, N. Scott, and D. L. Jackson for helpful discussions and to three anonymous reviewers for editorial corrections and helpful criticisms.

References

Bates, J. J., X. Wu, and D. Jackson, Interannual variability of upper-troposphere water vapor band brightness temperature, *J. Clim., 9,* 427-438, 1996.

Berk, A., L. Bernstein, and D. Robertson, Modtran: A moderate resolution model for lowtran 7, *GL-TR-89-0122,* Spectral Sci., Inc., Burlington, MA, 1989.

Bréon, F.-M., D. L. Jackson, and J. J. Bates, Evidence of atmospheric contamination on the measurement of the spectral response of the GMS-5 water vapor channel, *J. Atmos. Oceanic Technol., 16(11/2),* 1851-1853, 1999.

Bréon, F.-M., D. L. Jackson, and J. J. Bates, Calibration of the Meteosat water vapor channel using collocated NOAA/HIRS-12 measurements, *J. Geophys. Res., 105,* 11,925-11,933, 2000.

Chaboureau, J. P., A. Chédin, and N. Scott, Remote sensing of the vertical distribution of atmospheric water vapor from the TOVS observations: Method and validation, *J. Geophys. Res., 103,* 8743-8752, 1998.

Chédin, A., N. Scott, C. Wahiche, and P. Moulinier, The improved initialization inversion method: A high resolution physical method for temperature retrievals from the TIROS-N series, *J. Clim. Appl. Meteorol., 24,* 124-143, 1985.

Chevallier, F., F. Cheruy, N. A. Scott, and A. Chédin, A neural network approach for fast and accurate computation of a longwave radiative budget, *J. Appl. Meteorol., 37,* 1385-1397, 1998.

Elliott, W., and D. Gaffen, On the utility of radiosonde humidity archives for climate studies, *Bull. Am. Meteorol. Soc., 72,* 1507-1520, 1991.

Eyre, J., On systematic errors in satellite sounding products and their climatological mean values, *Q. J. R. Meteorol. Soc., 113,* 279-292, 1987.

Gaffen, D. J., and W. P. Elliott, Column Water Vapor Content in Clear and Cloudy Skies, *J. Clim., 6,* 2278-2287, 1993.

Kidwell, K. B., *NOAA Polar Orbiter Data User's Guide,* Natl. Oceanic and Atmos. Admin., Washington, D. C., 1991.

Malkmus, W., Random Lorentz model with exponential-tailed s^{-1} line intensity distribution function, *J. Opt. Soc. Am., 57,* 323-329, 1967.

Peixoto, J., and A. Oort *Physics of Climate,* 520 pp., Am. Inst. of Phys., New York, 1992.

Peixoto, J., and A. Oort, The climatology of relative humidity in the atmosphere, *J. Clim., 9,* 3443-3463, 1996.

Reuter, D., J. Susskind, and A. Pursch, First-guess dependence of a physically based set of temperature-humidity retrievals from HIRS2/MSU data, *J. Atmos. Oceanic Technol., 5,* 70-83, 1988.

Schmetz, J., An atmospheric-correction scheme for operational application to Meteosat infrared measurements, *ESA J., 10,* 145-159, 1986.

Schmetz, J., and O. Turpeinen, Estimation of the upper tropospheric relative humidity field from Meteosat water vapor image data, *J. Appl. Meteorol., 27,* 889-899, 1988.

Schmetz, J., C. Geijo, W. Menzel, K. Strabala, L. van de Berg, K. Holmlund, and S. Tjemkes, Satellite observations of upper tropospheric relative humidity, clouds and wind field divergence, *Beitr. Phys. Atmos., 68(4),* 345-357, 1995.

Scott, N., and A. Chédin, A fast line method for atmospheric absorption computations: the automatized atmospheric absorption atlas, *J. Appl. Meteorol., 20,* 802-812, 1981.

Scott, N., A. Chédin, R. Armante, J. Francis, C. Stubenrauch, J.-P. Chaboureau, F. Chevallier, and F. Cheruy, Characteristics of the TOVS pathfinder path-b data set, *Bull. Am. Meteorol. Soc., 80,* 2679-2701, 1999.

Soden, B., and F. Bretherton, Upper tropospheric relative humidity from GOES 6.7μm channel· Method and climatology for july 1987, *J. Geophys. Res., 98,* 16,669-16,688, 1993.

Soden, B., and J. Lanzante, An assessement of satellite and radiosonde climatologies of upper tropospheric water vapor, *J. Clim., 9,* 1235-1250, 1996

Sohn, B.J., J. Schmetz, S. Tjemkes, M. Koenig, H. Lutz, A. Arriaga, and E.S. Chung, Intercalibration of the Meteosat-7 water vapor channel with SSM/T-2, *J. Geophys. Res., 105,* 15,673-15,680, 2000.

Spencer, R., and W. Braswell, How dry is the tropical free troposphere? Implications for global warming theory, *Bull. Am. Meteorol. Soc., 78(6),* 1097-1106, 1997.

Stephens, G., D. Jackson, and L. Wittmeyer, Global observations of upper-tropospheric water vapor derived from TOVS radiance data, *J. Clim., 9,* 305-326, 1996.

Stubenrauch, C., N. Scott, and A. Chédin, Cloud field identification for earth radiation budget studies, part I, Cloud field classification using HIRS/TOVS sounder measurements, *J. Appl. Meteorol., 35(3),* 416-427, 1996.

Stubenrauch, C., A. Chédin, R. Armante, and N. Scott, Clouds as seen by satellite sounders (3I) and imagers (ISCCP), part II, A new approach for cloud parameter determination in the 3I algorithms, *J. Clim., 12,* 2214-2223, 1999.

Turpeinen, O., and J. Schmetz, Validation of the upper tropospheric relative humidity determined from Meteosat data, *J. Atmos. Oceanic Technol., 6(2),* 359-364, 1989.

van de Berg, L., A. Pyomjamsri, and J. Schmetz, Monthly mean upper tropospheric humidities in cloud-free areas from Meteosat observations, *Int. J. Clim., 11,* 819-826, 1991.

van de Berg, L., J. Schmetz, and J. Whitlock, On the calibration of the Meteosat water vapor channel, *J. Geophys. Res., 100,* 21,069-21,076, 1995.

Wahiche, C., N. A. Scott, and A. Chédin, Cloud detection and cloud parameters retrieval from the satellites of the TIROS-N series, *Ann. Geophys., 4(B2),* 207-220, 1986.

Werbowetzki, A., Atmospheric sounding user's guide, *NOAA Tech. Rep. NESS 83.*, Natl. Oceanic and Atmos. Admin., Washington, D. C., 1981.

J. J. Bates, NOAA/ERL-R/ET1A, Environmental Technology Laboratory, 325 Broadway, Boulder, CO 80303. (jbates@etl.noaa.gov)

A. Chédin, Laboratoire de Météorologie Dynamique, Ecole Polytechnique, 91128 Palaiseau Cedex, France. (chedin@jungle.polytechnique.fr)

C. Escoffier, Goddard Institute for Space Studies, Columbia University, 2880 Broadway, New York, NY 10025. (christel@giss.nasa.gov)

W. B. Rossow, NASA Goddard Institute for Space Studies, 2880 Broadway, New York, NY 10025. (wrossow @giss.nasa.gov)

J. Schmetz, EUMETSAT, Am Kavalleriesand 31, 64295 Darmstadt, Germany. (Schmetz@eumetsat.de)

(Received March 3, 2000; revised August 28, 2000; accepted September 7, 2000.)